

Article

Meteo-Climatic Conditions of Wind and Wave in the Perspective of Joint Energy Exploitation: Case Study of Dongluo Island, Hainan

Bo Li ^{1,2,3,*}, Junmin Li ^{1,2,3,*} , Wuyang Chen ¹, Junliang Liu ¹ and Ping Shi ^{1,3}

- ¹ State Key Laboratory of Tropical Oceanography, Key Laboratory of Science and Technology on Operational Oceanography, Guangdong Key Laboratory of Ocean Remote Sensing, South China Sea Institute of Oceanology, Chinese Academy of Sciences, Guangzhou 510301, China; chenwuyang@scsio.ac.cn (W.C.); lerry710@scsio.ac.cn (J.L.); pshi@scsio.ac.cn (P.S.)
- ² Sanya Institute of Oceanology, South China Sea Institute of Oceanology, Chinese Academy of Sciences, Sanya 572100, China
- ³ Southern Marine Science and Engineering Guangdong Laboratory (Guangzhou), Guangzhou 511458, China
- * Correspondence: libo@scsio.ac.cn (B.L.); jli@scsio.ac.cn (J.L.)

Abstract: Combined wind and wave power generation has advantages such as energy synergy and complementarity and will play a leading role in the integrated development of offshore renewable energy. From the perspective of joint energy development, this study focuses on the meteo-climatic wind and wave conditions in Dongluo Island, Hainan, in the South China Sea. Based on the concurrent measurement from in situ monitoring system, hourly data from June 2020 to September 2021 are used to reveal typical climate characteristics associated with the weak (inverse) correlation between wind and wave. The energy flux density of wind and wave are also assessed to describe the energy pattern. Principal component analysis (PCA) shows the wind parameters contribute a larger variance to the matrix of the wind–wave dataset than the waves, suggesting a lower stability of the wind climate. The first three components via PCA are then classified into five clusters to represent different climatic characteristics. Among them, the dominating cluster symbolizes a climatic circumstance with weaker winds and waves below normal. This cluster, evenly distributed in different seasons, shows the lowest wave–wind correlation, suggesting a favorable condition of the synergy of the two energies throughout the year. The clusters with the second and third largest sample sizes are mainly dominated in spring and winter, respectively. The magnitudes of the wind and wave parameters in these two clusters yield to a relation of “as one falls, another rises”, implying a high interest in complementarity between the two resources to a certain extent. The energy features inferred by meteo-climatic clusters are further verified by direct assessment of energy density. There are generally consistent variations between wind–wave climate and energy, both in magnitude and in seasonality. Based on these results, differentiated exploitation schemes considering the complementarity or synergy of wind and wave according to different seasons are recommended.

Keywords: wind and wave; climate; joint exploitation; synergy and complementarity; Dongluo Island



Citation: Li, B.; Li, J.; Chen, W.; Liu, J.; Shi, P. Meteo-Climatic Conditions of Wind and Wave in the Perspective of Joint Energy Exploitation: Case Study of Dongluo Island, Hainan. *Atmosphere* **2022**, *13*, 1076. <https://doi.org/10.3390/atmos13071076>

Academic Editor: Massimiliano Burlando

Received: 20 May 2022

Accepted: 5 July 2022

Published: 7 July 2022

Publisher's Note: MDPI stays neutral with regard to jurisdictional claims in published maps and institutional affiliations.



Copyright: © 2022 by the authors. Licensee MDPI, Basel, Switzerland. This article is an open access article distributed under the terms and conditions of the Creative Commons Attribution (CC BY) license (<https://creativecommons.org/licenses/by/4.0/>).

1. Introduction

Renewable marine energy, such as offshore wind and wave power, offers the advantages of being green, clean, and sustainable, as well as having a high energy density [1]. It is one of the most promising fossil fuel alternatives. Offshore wind energy is currently being installed in great capacity, while wave energy generation is still in its infancy. Incorporating the latter into wind farms is a way to encourage their growth [2]. In recent years, scientists have focused on the synergistic and complementary benefits of wind and wave resources, such as improving and stabilizing energy output, increasing predictability, sharing infrastructure costs, reducing intermittence, and maximizing spatial utilization [2–5], which

would play a leading role in the joint development of offshore renewable energy [6] and is regarded as a “game changer” for the industry [3].

In comparison to single-type energy development, hybrid systems prefer climate conditions of wind and wave with weak correlation and anti-correlation [7–9]. Under such conditions, wave energy and wind energy reach their peaks at different times, and alternating peaks and valleys mean synergistic advantage of multiple resources [3], which reduces the intermittency of a single resource [6,10]. Finding time–space windows with a low time correlation between wind and wave can help improve the efficiency of co-exploring the two resources [11].

The joint development of wind and wave energy is favored by sea areas with moderate and neutral resource density. In the Mediterranean, with moderate meteorology and sea state, scientists extracted the area related to a poor correlation between wind and wave [7,12]. For the first time, Wan et al. [13] assessed the joint development potential of the offshore wind and wave generation in the South China Sea (SCS), taking into account hybrid installed capacity. The latest study systematically evaluated the combinational potential in the coastal areas of South China considering the relationship between wind and wave energy [5], and the synergy and complementarity between the two resources in southern China were discussed for the first time. For example, the synergy of wind and wave energy is prominent with a high energy density of each other and a low correlation between them. If the density of one single energy source is not high enough, it can be used as a complement to another energy source with a higher density. Still, existing studies in the SCS have paid little attention to the climatic conditions from the perspective of joint development. Moreover, there is a lack of field observational studies on a targeted island in the South China coast. The SCS has a vast ocean basin and dense islands and reefs, as well as a genuine demand for utilization of wind and wave energy. It has a broad application prospect to establish an independent energy supply system for the island based on the multi-energy development.

Energy synergism of the wind and wave must be related to their climatic conditions [12]. The covariance of wind and wave at the climate level is a more fundamental scientific issue. By revealing the occurrence tendency and mechanism of independent changes of amplitude or direction of the wind and wave, it not only provides a basis for joint assessment of offshore renewable energy but also helps to understand the spatio-temporal characteristics and variation mechanism of wind and wave climate and enriches the knowledge system of climatic dynamics under different terrains. Clustering analysis has been employed to holistically describe climatic wind–wave conditions in the Mediterranean [7,12], the northwest Pacific coast [4], and the global ocean [14] from the standpoint of energy utilization. Environmental data are statistically examined in some of these studies to identify local and temporary circumstances of weak wind–wave correlation, hence promoting optimal sites for combined energy projects [7]. Furthermore, researchers created a process to determine the quality of the co-exploitation of the two energies using multivariate approaches on the meteorological data of wind and wave [12]. Recently, an integrated monitoring system was deployed on an uninhabited island, Dongluo Island, Hainan, in the northwestern SCS. Based on the observation data over 1 year, the density fluxes and availability of wind, wave, and tidal energies have been simultaneously assessed [15]. It is suggested that, for the energy development of the island, it is necessary to integrate and optimize the allocation of different types of marine energy. In this study, in the perspective of the combined exploration of offshore energies, the climate conditions and corresponding energy pattern of wind and wave power are further analyzed, and the potential periods conducive to joint energy development are screened. Usually, climate is the mean and variability of meteorological variables over a time spanning from months to millions of years [16]. Here, we use “meteo-climatic” to describe the general climate conditions based on a relatively short observation period of just over 1 year.

2. Data and Method

2.1. Data Gathering and Preprocess

Simultaneous observations of wind and waves were carried out on Dongluo Island, a small uninhabited island in the northwestern South China Sea (Figure 1). Real-time monitoring was conducted on the elements of the offshore wind field and waves at specific sites around the island. A MetPak weather station made by Gill Instruments Ltd. (Hampshire, UK) was deployed on the northeast coast of the island to measure the wind velocity and direction (red dot in Figure 1c). Concurrently, the wave parameters to the southeast of the island were observed by an acoustic wave and current profiler (AWAC) produced by Nortek Co. (Vangskroken 2, 1351 Rud, Norway) (blue dot in Figure 1c). A detailed description of the system can be referred to in [15].

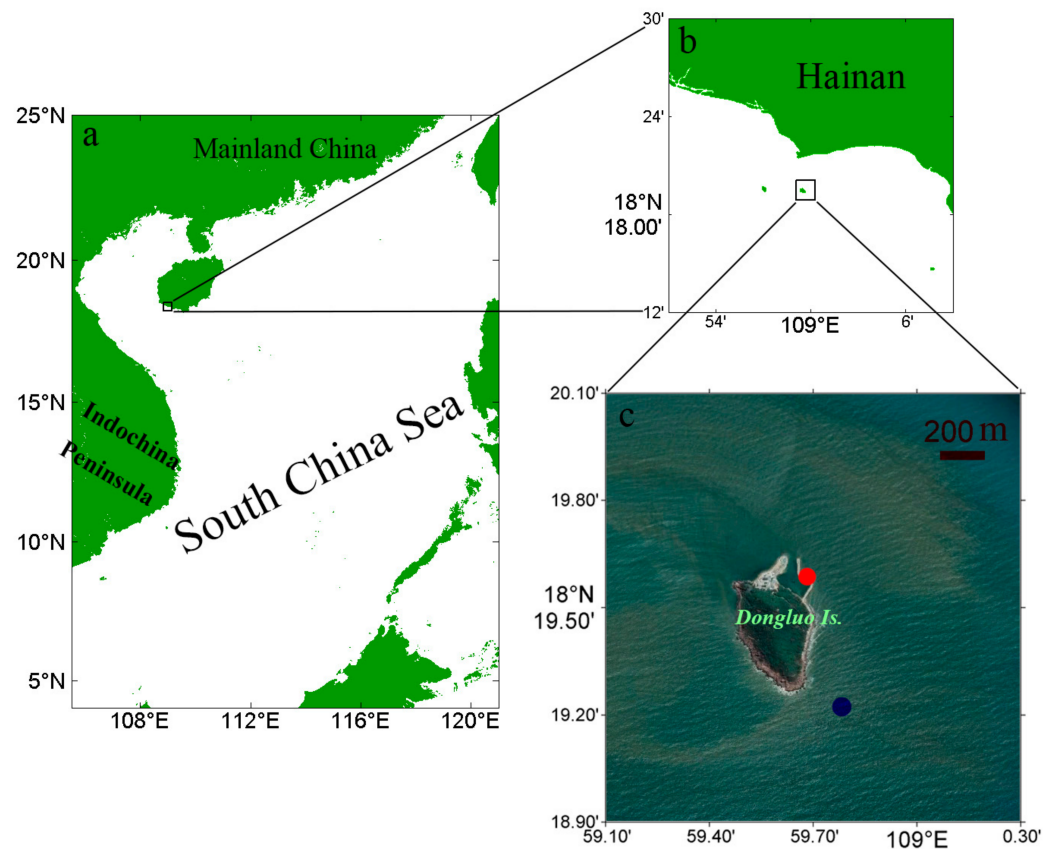


Figure 1. The geolocation of Dongluo Island in the SCS ((a) the area in the black box is zoomed-in) (b), relative to the Hainan coast (the area in the black box is zoomed-in), (c) and the hydro-meteorological monitoring station of the island (the red and blue dots are the meteorological and hydrological stations, respectively). The distance between the meteorological and hydrological stations is about 700 m.

Based on the AWAC of the monitoring system, the wave height, wave period, and wave directions were calculated using the wave spectra. The significant wave height (H_s) is defined as $H_s \equiv 4\sqrt{m_0}$, in which m_n is the n th moment of spectral density. Together with energy period (T_e), it can be used to determine the wave energy flux per unit of wave-crest length. The AWAC-observed wave period is not specified in terms of the T_e . Instead, T_e can be estimated by the formula $T_e = \alpha T_p$, where T_p is the peak period, and α is taken as 0.9, assuming that the sea state here is subjected to a standard JONSWAP spectrum [17]. The T_p observed by the AWAC is obtained from a parabolic fit around the discretized maximum of the two-dimensional wave spectrum. T_p could only assume discrete values because of the discretization of the wave spectrum in frequency space.

The wind energy flux is defined as the kinetic potential when the airflow crosses a section at a certain speed at 10 m above sea level. The Metpak weather station on the northeast coast of the island is installed at a height of 4 m, so the observed data need to be converted to u_{10} , which is the wind speed at 10 m above the sea level in the unit of m/s by [18,19]:

$$u_{10} = \frac{u(z)}{1 + \frac{\sqrt{Cd_{10}}}{0.4} \times \ln\left(\frac{z}{10}\right)} \tag{1}$$

where $z = 4$ m, which is the height of the wind sensor; $u(z)$ is the wind speed measured by the wind sensor; and $Cd_{10} = 0.0011$ is the drag coefficient.

The sampling frequencies of the AWAC and Metpak are 30 min and 1 s, respectively. In this study, the wind and wave parameters are averaged every 1 h, and 9691 concurrent samples of wind field and waves around Dongluo island from 12 June 2020 to 9 September 2021 were obtained. The wind and wave directions are averaged by the angle averaging method.

2.2. Assessment Method of Two Offshore Resources

Wind energy is defined as the kinetic potential that the airflow crosses a section [13,20–22]. Thus, wind energy density passing through a unit area is calculated as follows:

$$J = 0.5\rho_a u_{10}^3 \tag{2}$$

where J is wind power density in $W\ m^{-2}$, ρ_a is the air density taken as $1.293\ kg\ m^{-3}$, and u_{10} is the wind speed at 10 m above the mean sea level in the unit of $m\ s^{-1}$.

According to the wave energy resource assessment algorithms by Cornett [17], the wave energy density is calculated by:

$$P = \frac{\rho_w g^2}{64\pi} Hs^2 Te \tag{3}$$

where P is the wave energy density flux per unit of wave-crest length ($kW\ m^{-1}$), Hs is in m, and Te is in s. Furthermore, ρ_w is the density of seawater as $1025\ kg\ m^{-3}$, and g is the gravitational acceleration as $9.8\ m\ s^{-2}$.

The wave energy stability is quantified by the coefficient of variation (Cv) by the formula [15,17]:

$$Cv = \left[\frac{\sum_{i=1}^N (P_i - \bar{P})^2}{N} \right]^{1/2} / \bar{P} \tag{4}$$

where \bar{P} is the mean of P_i , and N is the sample size of P_i . The same method is adopted in the estimation of the Cv of wind energy J .

Wen et al. [5] recently proposed a new method to evaluate the complementarity and synergy potential based on the occurrence rate of offshore wind and wave resources above their respective electrical generation threshold (EGT). They suggested the EGT of $80\ W\ m^{-2}$ and $2.5\ kW\ m^{-1}$ for wind and wave energies, respectively. In general, the EGT of $2\ kW\ m^{-1}$ is more widely used in the SCS for wave harvesting, e.g., [13,15,20]. As a result, the indices of wind complemented by wave energy (WICWA), wave energy complemented by wind energy (WACWI), and higher and lower densities for both wind and wave energy (WIWA_H, WIWA_L) are defined to describe the joint energy patterns using the following:

$$\begin{cases} WICWA = \frac{n(J \leq 80\ Wm^{-2}, P \geq 2\ kWm^{-1})}{N} \times 100\% \\ WACWI = \frac{n(J \leq 80\ Wm^{-2}, P \geq 2\ kWm^{-1})}{N} \times 100\% \\ WIWA_H = \frac{n(J \geq 80\ Wm^{-2}, P \geq 2\ kWm^{-1})}{N} \times 100\% \\ WIWA_L = \frac{n(J \leq 80\ Wm^{-2}, P \geq 2\ kWm^{-1})}{N} \times 100\% \end{cases} \tag{5}$$

where n is the size of samples in which J and P satisfy the corresponding criteria, and N is the total sample size. A higher WICWA, WACWI, or WIWA_H indicates a considerable synergy

potential for joint exploration of wind and wave energy [5]. This definition emphasizes the magnitude of the density flux between the two energies, ignoring the characteristic of co-variation within them. In this study, high synergy is referring in particular to the energy pattern with a weak/anti-relationship between two resources.

2.3. Statistical Method

There is an interest in co-exploiting the two types of offshore energies where the wind and wave energy yield to lower correlations. According to the Pearson's correlation coefficient, the time correlation between wind and wave parameters is investigated:

$$r = \frac{1}{N} \sum_{k=1}^N \frac{[x(k) - \mu_x][y(k) - \mu_y]}{\sigma_x \sigma_y} \quad (6)$$

where μ_x , μ_y , σ_x , σ_y are the mean and the standard deviation of the variables x and y of k observations, and N is the total sample size.

The meteo-climatic condition was analyzed based on the multivariate matrix of wind-wave parameters, including the wind speed (Wsp), wind direction ($Winddir$), significant wave height (Hs), peak wave period (Tp), and wave direction ($Wavedir$). Because the statistic value of the wind direction is unstable, i.e., has a runout near the north direction (0° or 360°) (Figure 2b), the wind vector is decomposed into its zonal and meridional components (U , V) for further analysis. The principal components analysis (PCA) is used to reduce the dimension of the matrix, and the key parameter combinations of principal components (PCs) are extracted at the time scale of an hour. The number of principal components is determined using the "eigenvalue larger than 1" criterion, which means that all components that explain less than the variance of one of the original variables are eliminated. This method allows for the selection of a few components to explain the entire dataset with minimal loss of original information.

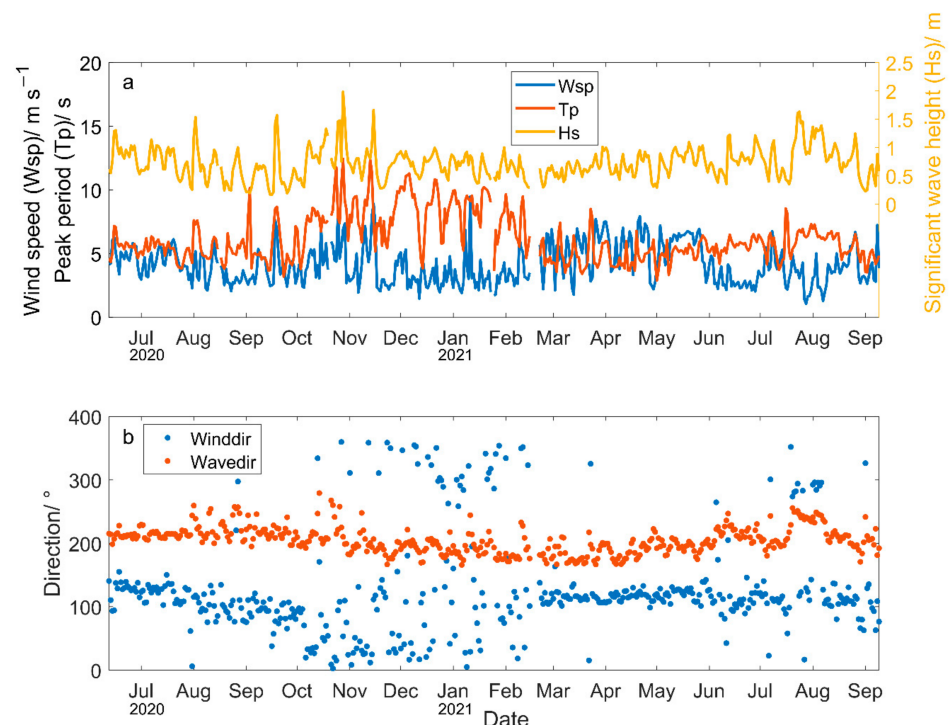


Figure 2. Daily series of the wind speed (Wsp), peak wave period (Tp), and significant wave height (Hs) (a) and mean wind/wave directions (b).

To examine the similarities of meteo-climatic data groupings, the dimension-reduced samples are further separated using cluster analysis (CA). The factor scores (loadings) produced via PCA extraction are subjected to a K-means CA. The climate characteristics

and corresponding synergy level of wind and waves of different clusters are evaluated. That procedure partitions the points in the data matrix into K clusters. This partition minimizes the sum, over all clusters, of the within-cluster sums of point-to-cluster-centroid distances. The Euclidean distance is chosen as the distance measurement:

$$d(x_i, y_i) = \sqrt{\sum_{k=1}^n (x_{ik} - y_{ik})^2} \tag{7}$$

where x_i and y_i are i th coordinates of the k th dimensional space.

For the aim of this study, K-means CA was run three times: the later cluster centroids of the solution obtained after the former run were used as initial centers in the later run. The results presented here are hence related to the third run.

3. Result and Discussion

3.1. Wind and Wave Conditions

The stability of and temporal variability in the energy flux affect the possibilities for the integrated utilization of different energy sources [10]. The temporal variability in wind–wave energy is statistically described. It can be observed that wind and wave patterns are characterized by a certain degree of seasonality (Figure 2). However, different parameters of the wind and waves do not show a similar variation trend. Statistical analysis indicates that temporal patterns of wind and waves are generally poorly correlated (Table 1). These conditions are of interest in the perspective of reducing the overall variability in the produced power.

Table 1. Correlation analysis between wind and wave. N = 9691.

	<i>Hs</i>	<i>Tp</i>	<i>Wavedir</i>	<i>Wsp</i>	<i>U</i>
<i>Hs</i>	1				
<i>Tp</i>	0.253 **	1			
<i>Wavedir</i>	0.204 **	0.064 **	1		
<i>Wsp</i>	0.345 **	−0.130 **	−0.215 **	1	
<i>U</i>	0.108 **	−0.252 **	−0.320 **	0.624 **	1
<i>V</i>	−0.130 **	0.408 **	0.152 **	−0.234 **	−0.237 **

** Correlation at the confidence level of 99%.

The PCA shows that the first three components (eigenvalue higher than 1) explain 76.48% of the original variance in the wind–wave dataset (Figure 3). According to the loading of each variation in the different components, the first component (PC1) mainly accounts for *Wsp* and *U*, the second component (PC2) accounts for *Hs* and *Tp*, while the third component (PC3) accounts for just the wave direction and *V* (Table 2). Wind parameters contribute most to the variance in the meteo-climate conditions of the island. That is, the variance in the wave parameters is less than the wind parameters.

3.2. Classification of the Meteo-Climatic Conditions

The matrix of the first three components via PCA is subjected to the CA. Five clusters are classified to represent the different meteo-climatic characteristics of wind–wave conditions (Figure 4). For cluster 1, the PC1 (*Wsp*, *U*) and PC2 (*Hs*, *Tp*) significantly exceed the averages, representing an energy-extensive meteo-climatic condition. The degree of wave direction in PC3 is slightly larger than the average (~210°, corresponding to SW, Figure 2b) and indicates waves from the west. In addition, a below-average *V* is shown in PC3 (notice the ‘-’ sign in front of *V*). Cluster 2 represents a decreased *Wsp* to below average and increased *Hs* and *Tp* to above average in the first two PCs, suggesting a swell-dominated sea state with the weakened local wind. Meanwhile, the PC3 of this cluster indicates that the swell may be from the west or northwest direction, with a significantly weakened meridional wind. The samples in cluster 3 suggest a calm sea state with an average wave direction of 210°. Illustrated in cluster 4 are higher offshore wind with moderate wave

height and wave period, as well as a southwest wave direction closer to average. Similar to cluster 2, cluster 5 indicates a high sea state dominated by swell with weakened wind energy. However, as suggested by the average-below wave direction in PC3, the swell in this cluster is mainly from the east or northeast. The meridional wind velocity of cluster 5 is above average, suggesting that the weakened *Wsp* mainly results from the significant decrease in its zonal component.

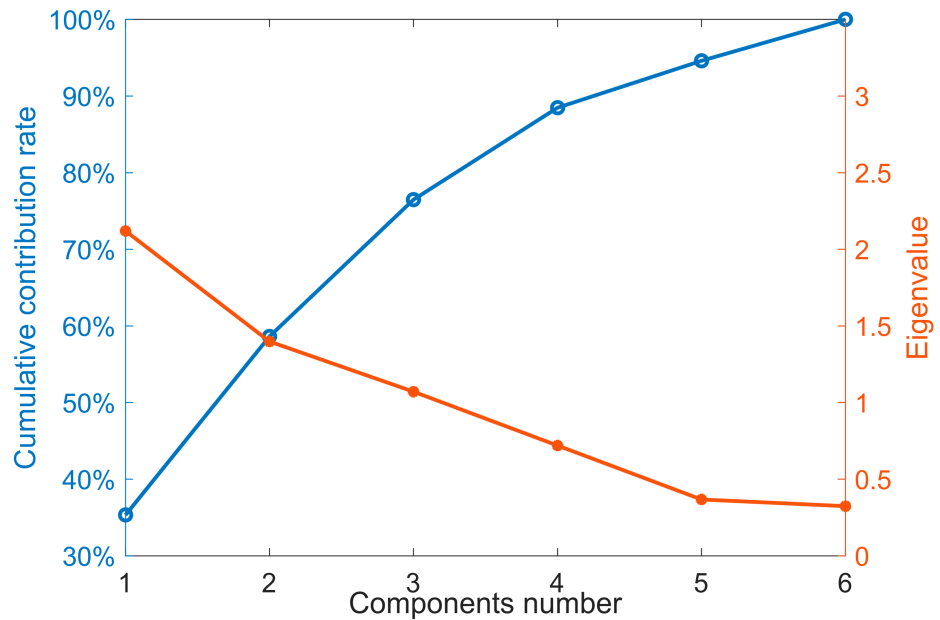


Figure 3. The cumulative contribution rate of the principal components and their corresponding eigenvalues. The first three components present an eigenvalue higher than 1. Only these are considered in further analysis.

Table 2. Factor loadings of the PCA. Higher correlations exceeding 0.5 are exhibited.

Component	1	2	3
Contribution rate	35.33%	23.31%	17.85%
Eigenvalue	2.12	1.40	1.07
Loading	<i>Hs</i>	0.722	
	<i>Tp</i>	0.512	
	<i>Wavedir</i>		0.634
	<i>Wsp</i>	0.540	
	<i>U</i>	0.564	
	<i>V</i>		−0.518

Among these clusters, cluster 1 is the most favorable meteo-climatic condition for single energy exploration for both wind and wave energy. However, as indicated in Figure 4b, the samples of cluster 1 are too sparse and discrete, which is inconducive for the continuity and stability of single energy output. So, a joint exploration scheme combining wind and wave energies may be preferred.

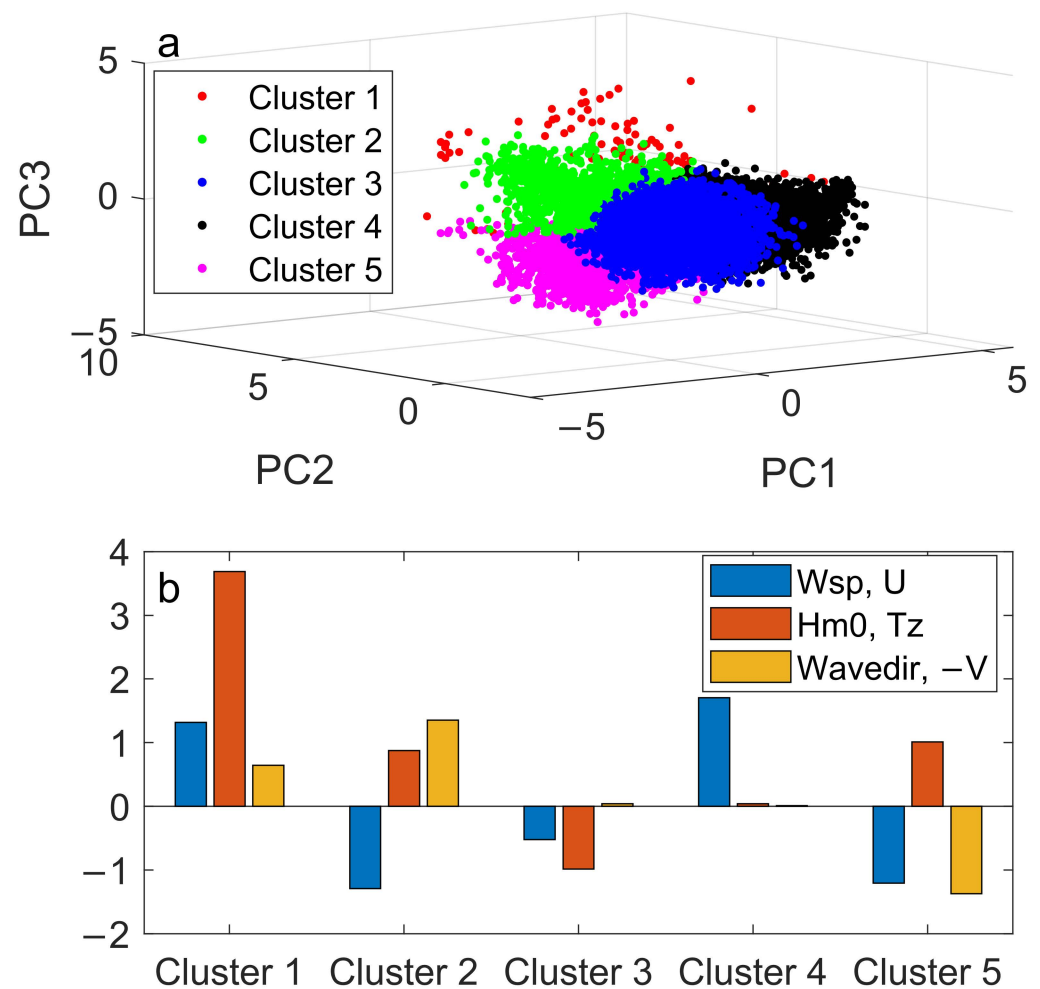


Figure 4. Scatter diagram of the classification of the first three PCs of wind-wave dataset (a) and the standardized characteristics of each cluster (b).

The correlations between the wind and wave parameters obtained by pooling the entire dataset (reported in Table 1) and the ones obtained after splitting the dataset into the different clusters are compared in Table 3. In general, correlation coefficients between the H_s and W_{sp} among different clusters are rather low, suggesting a potential condition of joint development. A previous study indicated that the correlation coefficients between the monthly H_s in the adjacent water of Dongluo Island with the W_{sp} in the western Luzon strait region exceed 0.9, while that with the W_{sp} at the corresponding grid point is about 0.75 [23]. It is suggested that the study area is strongly influenced by swell propagation from remote seas. Westward swells induced by the gales that occur in the northeast of the South China Sea result in the variations in H_s in the study area. Furthermore, the topography of the island may also affect the relationship between local wind and waves [15,24].

Cluster 3 shows the lowest correlation coefficient of 0.050 between W_{sp} and H_s , and the largest negative correlation coefficient of -0.229 between W_{sp} and T_p . Meanwhile, the wind energy density is anti-related with wave energy (correlation coefficient is -0.076), the only negative correlation coefficient between J and P among all clusters. In addition, the sample size of cluster 3 is the largest among all clusters, suggesting a wide time window of co-exploring potential. It should be noted that the strength of the wind and wave in cluster 3 is lower than the average of the whole samples; that is, the wind and wave cluster with the highest irrelevant/anti-correlation level may be weak in energy output. The meteorological characteristic of other clusters also needs to be considered, making optimal use of in situ measurements to characterize the resources of coastal sites of the island. For example, there is a seesaw phenomenon of “as one falls, another rises” between wind and wave

parameters in clusters 2, 4, and 5. This may indicate the complementary effect between the two energies.

Table 3. Correlation coefficient between wind and wave parameters and the energy density of different clusters.

		<i>Hs</i>	<i>Tp</i>	<i>Wsp</i>	<i>p</i>
Cluster 1 N = 217	<i>Hs</i>	1	0.486 **	0.143 *	0.153 *
	<i>Tp</i>		1	0.138 *	
	<i>J</i>				
Cluster 2 N = 1292	<i>Hs</i>	1	0.155 **	0.154 **	0.187 **
	<i>Tp</i>		1	−0.031	
	<i>J</i>				
Cluster 3 N = 3514	<i>Hs</i>	1	0.208 **	0.050 **	−0.076 **
	<i>Tp</i>		1	−0.229 **	
	<i>J</i>				
Cluster 4 N = 3080	<i>Hs</i>	1	0.461 **	0.319 **	0.202 **
	<i>Tp</i>		1	−0.126	
	<i>J</i>				
Cluster 5 N = 1588	<i>Hs</i>	1	−0.106 **	0.226 **	0.241 **
	<i>Tp</i>		1	−0.053 *	
	<i>J</i>				
Total N = 9691	<i>Hs</i>	1	0.253 **	0.345 **	0.287 **
	<i>Tp</i>		1	−0.130 **	
	<i>J</i>				

* Correlation at the confidence level of 95%. ** Correlation at the confidence level of 99%.

Statistical analysis of the synergy potential of the two energies is shown in Table 4. As Wen et al. defined [5], considering the density of the two energies, the first three patterns (WICWA, WACWI, and WIWA_H) in the table indicate considerable potential of combining wind and wave energy. However, the total frequency of these situations is just 49.77%. Half of the sampling capacity is subjected to a low wind and wave energy pattern (WIWA_L). The high value of WIWA_L (50.13%) indicates a high frequency of insufficient offshore energy near Dongluo Island coast. In this situation, the wind and wave energies both show a lower density and a relatively higher *Cv*, which is not feasible for single energy development. However, the correlation coefficient of the *J* and *P* corresponding to the WIWA_L energy pattern is 0.045, which is the lowest among all patterns exceeding the 95% confidence level, suggesting the superposition of energy caused by the asynchronous variation in the two energies.

The combined energy patterns between the two resources of different meteo-climatic clusters are illustrated in Figure 5. The meteo-climatic patterns generally coincide with the energy pattern. The energy pattern of WIWA_H contributes most (89%) to the sample of cluster 1, where both PC1 (*Wsp, U*) and PC2 (*Hs, Tp*) exceed their averages. For clusters 2 and 5, there are decreased *Wsp* values to below average and increased *Hs* and *Tp* values to above average, and the energy patterns of WACWI and WIWA_L are remarkable. Compared to these two clusters, there are opposite meteo-climatic characteristics and energy patterns in cluster 4. For cluster 3, whose sampling capacity is the largest, the strength of *Wsp, Hs*, and *Tp* are lower than their respective averages in the whole sample, and the highest percentage of 96% is contributed to by the energy pattern of WIWA_L.

Table 4. Synergy aspects of the two resources.

	Value via Formula (5)	J ($W\ m^{-2}$)		P ($kW\ m^{-1}$)		$r(J, p)$
		Mean	Cv	Mean	Cv	
WICWA ($J > 80, p < 2$) N = 1954	20.16%	166.043	0.5043	1.091	0.450	0.317 **
WACWI ($J < 80, p > 2$) N = 1629	16.81%	24.457	0.930	3.515	0.566	0.030
WIWA _H ($J > 80, p > 2$) N = 1250	12.90%	217.591	0.652	4.244	1.024	0.259 **
WIWA _L ($J < 80, p < 2$) N = 4858	50.13%	25.830	0.850	0.789	0.685	0.045 **
Total N = 9691	100%	78.604	1.289	1.754	1.297	0.287 **

** Correlation at the confidence level of 99%.

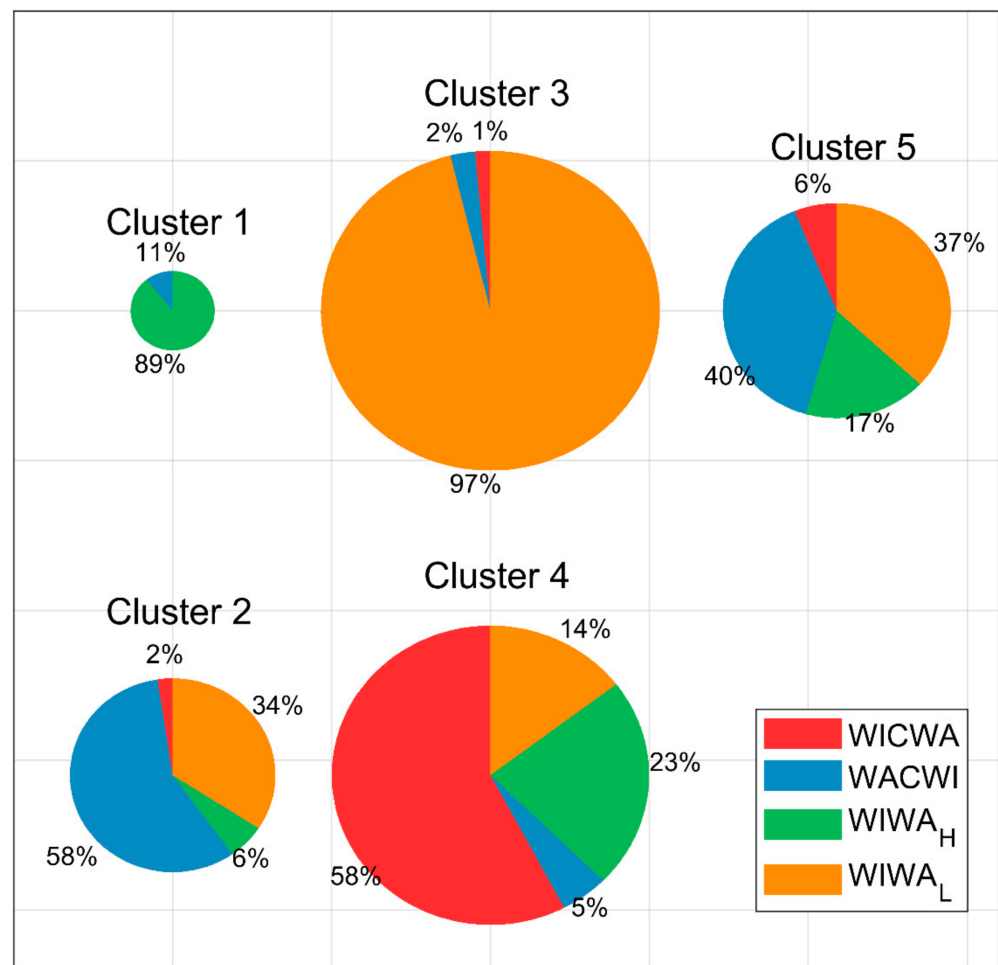


Figure 5. Energy patterns between the two resources of different meteo-climatic clusters. The disc area indicates sampling size of each cluster. The colored sectors of each disc are the percentage of the synergy categories.

The frequency distribution of the clusters according to month is shown in Figure 6. The occurrence frequency of cluster 1 is rather low, so this study focuses on the last four clusters. Cluster 3 accounts for a considerable proportion (16.4–65.19%) every month during the whole observed period, while the other clusters show a significant monthly variation. The proportions of clusters 2, 4, and 5 indicate a sharp increase in some months. For example, clusters 4 and 5 predominate from March to May and from October to January, respectively, while from July to August, the prevailing cluster is cluster 2.

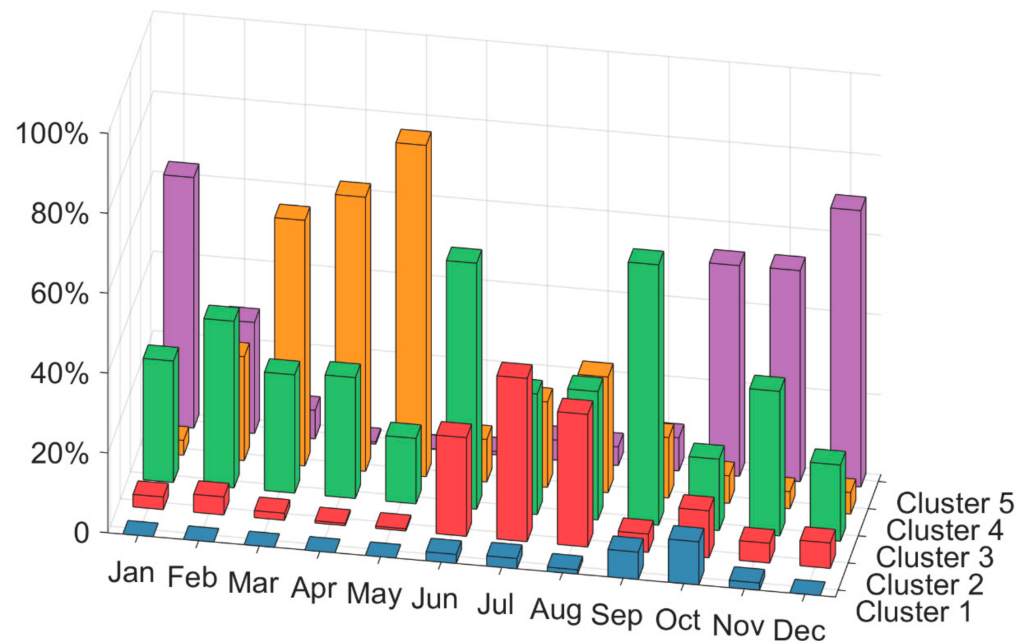


Figure 6. Frequency distribution of the meteo-climatic clusters according to month (June 2020 to September 2021).

The annual samples from September 2020 to August 2021 are selected to illustrate the seasonal frequency distribution according to the meteo-climatic clusters (Figure 7a) and energy patterns (Figure 7b). Among all five clusters, cluster 3 accounts for the highest percentage of 34.5%, which is uniformly distributed annually. Its corresponding energy pattern of $WIWA_L$ also shows a maximum proportion and a well-distributed seasonal frequency. In addition, clusters 4 (28.2%) and 5 (23.6%) account for the second and the third largest sampling sizes, respectively. However, the sample capacities of these two clusters show significant seasonality. Cluster 4 during spring and cluster 5 during winter should be particularly considered in the combination of wind and wave energy. Cluster 2 (accounts for 11.5% of all clusters), which has a similar meteo-climatic characteristic (extensive wave and weakened wind) to cluster 5, is more distributed in summer. Generally speaking, in spring, the dominating cluster (cluster 4) shows a strengthened wind and an averaged wave, which may be favored by the potential of wind resources complementing wave resources (WICWA) to a certain extent. During winter and summer, the respectively preponderant clusters (clusters 5 and 2) show an extensive wave height and wave period, and a weakened wind speed, which implies the potential of wave resources complemented by wind resources (WACWI). Consequently, the energy pattern of WICWA is dominated in spring, and the WACWI pattern is more likely to occur in winter and summer. So, differentiated exploring schemes should be considered according to the complementarity or synergy of wind and wave during different seasons.

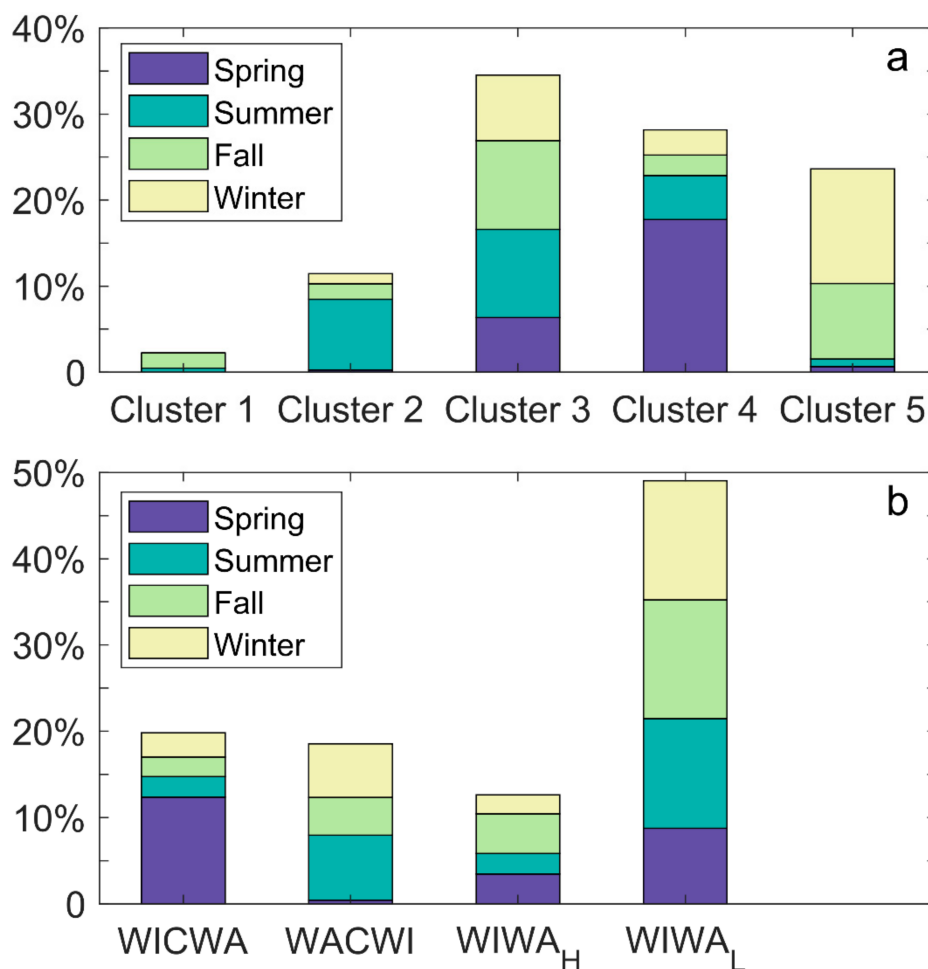


Figure 7. Seasonal frequency distribution according to the meteo-climatic clusters (a) and energy patterns (b) (September 2020 to August 2021).

4. Conclusions

From the perspective of combined exploring of the offshore energies, the meteo-climatic conditions and corresponding energy pattern of the wind and wave of Dongluo Island, Hainan, China, are analyzed in this study. The concurrent measurement of wind and wave parameters is gathered based on a hydro-meteorological monitoring system in the coastal area of the island, and 15 months of data were collected from June 2020 to September 2021. The wind speed (Wsp) and its zonal and meridional components (U , V), the significant wave height (Hs), the peak wave period (Tp), and the mean wave direction ($Wavedir$) are averaged every 1 h for time-matching, and a multi-variable matrix of these parameters is obtained for further analysis. Using principal component analysis (PCA) and K-means cluster analysis (CA), the matrix is reduced dimensionally and then classified into several clusters to describe meteo-climatic characteristics of the wind and waves. The energy densities of wind and wave resources according to different meteo-climatic clusters are evaluated. The combined energy patterns of the two resources are diagnosed. Finally, differentiated exploring schemes according to different seasons are recommended.

The results show that the Wsp and U contribute most to the first component, while the Hs and Tp mainly contribute to the second one. The matrix of the first three components via PCA is subjected to the CA. Five clusters are classified to represent different climatology of the wave and wind. It is noted that the correlation coefficients between Wsp and Hs (Tp) are rather low in all clusters, and the meteo-climatic condition around Dongluo Island shows a certain potential for the joint development of offshore wind and wave energy.

For the cluster with the highest frequency (which accounts for 34.54% of all samples), the wind and wave intensities are below their average values of the whole sample. However, these samples show the lowest correlation coefficient of 0.050 between Wsp and Hs and the largest negative correlation coefficient of -0.229 between Wsp and Tp . That is, the dominated cluster shows a lower correlation between wave and wind, suggesting the more favourable condition of a synergistic effect of the two energies. What is more, samples of this cluster are evenly distributed in different seasons, which is worthy of consideration in joint energy development.

The clusters with the second and third largest sample sizes are mainly dominated in spring and winter, respectively. In spring, the Wsp is significantly higher than the average level, while the Hs and Tp are generally equal to the average level, suggesting a higher probability of wind resources complemented by wave resources to some extent. In winter, the Wsp is lower than its average, while the Hs and Tp are significantly higher than their average values, which might be suitable for the collaborative development mode of wave-dominated and wind supplemented. As a result, differentiating exploration schemes based on the complementarity or synergy of wind and wave energy throughout different seasons should be considered.

The above energy distribution features inferred by meteo-climatic clusters are verified by a direct evaluation of the energy density. The synergy between wind and wave energy is closely tied to their climatic circumstances. There are consistent variations between wind–wave climate and energy both in amplitude and seasonality. It is suggested that wind–wave covariance at the meteo-climatic level can indicate a joint potential of offshore energy by revealing the occurrence tendency and variation in amplitude or direction of the wind and wave.

It is noted that the joint energy exploitation potential presented in this paper is specific to the considered site. Further measurements or studies should be carried out for accessing the joint energy potential of other sites along the island. In addition, Dongluo Island is close to landmass, so marine energy here may be utilized to complement conventional fuel or the mainland's power grid. Small-scale and low-investment installation would meet the demand. However, in the case of distant islands far out at sea, their isolated grid connection emphasizes the need for renewable energies in achieving energy self-sufficiency. In such an environment, large-scale offshore energy installations are preferable. As a result, in addition to the two resources' climatic and energy synergy, more synergism in legislative (e.g., common regulatory framework, maritime spatial planning, simplified licensing procedure) and project or technology areas (e.g., shared logistics, common infrastructure investment, environmental benefits) [2] should be considered in co-exploration programming.

Author Contributions: Conceptualization, B.L.; methodology, B.L.; software, W.C.; validation, W.C.; formal analysis, J.L. (Junliang Liu); investigation, B.L.; resources, J.L. (Junliang Liu); data curation, B.L.; writing—original draft preparation, B.L.; writing—review and editing, J.L. (Junmin Li); visualization, B.L.; supervision, J.L. (Junmin Li); project administration, J.L. (Junmin Li) and P.S.; funding acquisition, P.S. All authors have read and agreed to the published version of the manuscript.

Funding: This study is supported by the Hainan Provincial Natural Science Foundation of China (421QN380), Guangzhou Science and Technology Project (202102020464), the Key Special Project for Introduced Talents Team of Southern Marine Science and Engineering Guangdong Laboratory (Guangzhou) (GML2019ZD0302), the Science and Technology Planning Project of Guangdong Province of China (2021B1212050023), and the CAS Key Laboratory of Science and Technology on Operational Oceanography (OOST2021-02).

Data Availability Statement: The data are available from the corresponding author by request.

Acknowledgments: The numerical calculation is supported by the High-Performance Computing Division in the South China Sea Institute of Oceanology.

Conflicts of Interest: The authors declare no conflict of interest.

References

1. Borthwick, A.G.L. Marine renewable energy seascape. *Engineering* **2016**, *2*, 69–78. [CrossRef]
2. Pérez-Collazo, C.; Greaves, D.; Iglesias, G. A review of combined wave and offshore wind energy. *Renew. Sustain. Energy Rev.* **2015**, *42*, 141–153. [CrossRef]
3. Albert, L. *Wave and Wind Are the New Hybrid Renewable Energy Source*; Seabased: Uppsala, Sweden, 2020; Available online: <https://seabased.com/news-insights/wave-and-wind-are-the-new-hybrid-renewable-energy-source> (accessed on 7 July 2020).
4. Robertson, B.; Dunkle, G.; Gadasi, J.; Garcia-Medina, G.; Yang, Z. Holistic marine energy resource assessments: A wave and offshore wind perspective of metocean conditions. *Renew. Energy* **2021**, *170*, 286–301. [CrossRef]
5. Wen, Y.; Kamranzad, B.; Lin, P. Joint exploitation potential of offshore wind and wave energy along the south and southeast coasts of China. *Energy* **2022**, *249*, 123710. [CrossRef]
6. Rasool, S.; Muttaqi, K.M.; Sutanto, D.; Hemer, M. Quantifying the reduction in power variability of co-located offshore wind-wave farms. *Renew. Energy* **2022**, *185*, 1018–1033. [CrossRef]
7. Azzellino, A.; Lanfredi, C.; Riefole, L.; De Santis, V.; Contestabile, P.; Vicinanza, D. Combined exploitation of offshore wind and wave energy in the Italian Seas: A spatial planning approach. *Front. Energy Res.* **2019**, *7*, 42. [CrossRef]
8. Ferrari, F.; Besio, G.; Cassola, F.; Mazzino, A. Optimized wind and wave energy resource assessment and offshore exploitability in the Mediterranean Sea. *Energy* **2020**, *190*, 116447. [CrossRef]
9. Lira-Loarca, A.; Ferrari, F.; Mazzino, A.; Besio, G. Future wind and wave energy resources and exploitability in the Mediterranean Sea by 2100. *Appl. Energy* **2021**, *302*, 117492. [CrossRef]
10. Widén, J.; Carpmann, N.; Castellucci, V.; Lingfors, D.; Olauson, J.; Remouit, F.; Bergkvist, M.; Grabbe, M.; Waters, R. Variability assessment and forecasting of renewables: A review for solar, wind, wave and tidal resources. *Renew. Sustain. Energy Rev.* **2015**, *44*, 356–375. [CrossRef]
11. Astariz, S.; Iglesias, G. The collocation feasibility index—A method for selecting sites for co-located wave and wind farms. *Renew. Energy* **2017**, *103*, 811–824. [CrossRef]
12. Contestabile, P.; Russo, S.; Azzellino, A.; Cascetta, F.; Vicinanza, D. Combination of local sea winds/land breezes and nearshore wave energy resource: Case study at MaRELab (Naples, Italy). *Energy Convers. Manag.* **2022**, *257*, 115356. [CrossRef]
13. Wan, Y.; Fan, C.; Dai, Y.; Li, L.; Sun, W.; Zhou, P.; Qu, X. Assessment of the joint development potential of wave and wind energy in the South China Sea. *Energies* **2018**, *11*, 398. [CrossRef]
14. Fairley, I.; Lewis, M.; Robertson, B.; Hemer, M.; Masters, I.; Horrillo-Caraballo, J.; Karunarathna, H.; Reeve, D.E. A classification system for global wave energy resources based on multivariate clustering. *Appl. Energy* **2020**, *262*, 114515. [CrossRef]
15. Li, B.; Chen, W.; Li, J.; Liu, J.; Shi, P. Integrated monitoring and assessments of marine energy for a small uninhabited island. *Energy Rep.* **2022**, *8*, 63–72. [CrossRef]
16. Planton, S. (Ed.) IPCC Annex III: Glossary. In *Climate Change 2013: The Physical Science Basis. Contribution of Working Group I to the Fifth Assessment Report of the Intergovernmental Panel on Climate Change*; Cambridge University Press: Cambridge, UK; New York, NY, USA, 2013; Available online: https://web.archive.org/web/20160524223615/http://www.ipcc.ch/pdf/assessment-report/ar5/wg1/WG1AR5_AnnexIII_FINAL.pdf (accessed on 4 July 2022).
17. Cornett, A.M. A global wave energy resource assessment. In *Proceedings of the 18th International Conference on Offshore and Polar Engineering*, Vancouver, BC, Canada, 6–11 July 2008; The International Society of Offshore and Polar Engineers: Vancouver, BC, Canada, 2008; Volume 1, pp. 318–326.
18. Large, W.G.; Pond, P. Open ocean momentum flux measurements in moderate to strong winds. *J. Phys. Oceanogr.* **1981**, *11*, 324–336. [CrossRef]
19. Sutton, A.J.; Wanninkhof, R.; Sabine, C.L.; Feely, R.A.; Cronin, M.F.; Weller, R.A. Variability and trends in surface seawater pCO₂ and CO₂ flux in the Pacific Ocean. *Geophys. Res. Lett.* **2017**, *44*, 5627–5636. [CrossRef]
20. Zheng, C.W.; Pan, J.; Li, J.X. Assessing the China Sea wind energy and wave energy resources from 1988 to 2009. *Ocean Eng.* **2013**, *65*, 39–48. [CrossRef]
21. Chen, X.; Wang, K.; Zhang, Z.; Zeng, Y.; Zhang, Y.; O’Driscoll, K. An assessment of wind and wave climate as potential sources of renewable energy in the nearshore Shenzhen coastal zone of the South China Sea. *Energy* **2017**, *134*, 789–801. [CrossRef]
22. Wang, Z.; Duan, C.; Dong, S. Long-term wind and wave energy resource assessment in the South China sea based on 30-year hindcast data. *Ocean Eng.* **2018**, *163*, 58–75. [CrossRef]
23. Wang, H.; Fu, D.; Liu, D.; Xiao, X.; Liu, B. Analysis and prediction of significant wave height in the Beibu Gulf, South China Sea. *J. Geophys. Res. Ocean.* **2021**, *126*, e2020JC017144. [CrossRef]
24. Li, B.; Li, J.; Liu, J.; Tang, S.; Chen, W.; Shi, P.; Liu, Y. Calibration experiments of CFOSAT wavelength in the Southern South China Sea by artificial neural networks. *Remote Sens.* **2022**, *14*, 773. [CrossRef]